ARTICLE INFO
Article ID: 03-18-01-0001

doi:10.4271/03-18-01-0001

Premixed Dual-Fuel Combustion of *Camelina sativa* Oil and Ethanol

Grzegorz Pawlak,[1] Tomasz Skrzek,[2] Krzysztof Kosiuczenko,[1] Patryk Płochocki,[1] and Przemysław Simiński[1]

[1]Military Institute of Armored and Automotive Technology, Poland
[2]Kazimierz Pulaski University of Radom, Faculty of Mechanical Engineering, Poland

Abstract

Dual-fuel (DF) engines enable efficient utilization of a low reactivity fuel (LRF), usually port-injected, and a high reactivity fuel (HRF) provided directly into the cylinder. Ethanol and *Camelina sativa* oil can be ecologically effective but not fully recognized alternatives for energy production using modern CI engines equipped with a common rail system and adopted for dual fueling. The high efficiency of the process depends on the organization of the combustion.

The article describes the premixed dual-fuel combustion (PDFC) realized by dividing the *Camelina sativa* dose and adjusting its injection timing to the energetic share of ethanol in the DF mixture. The injection strategy of HRF is crucial to confine knock, which limits DF engine operation, but the influence of EGR is also important. The research AVL engine's dual-fueling tests focused on combustion process modification by the proposed injection strategy and cooled EGR at different substitution rates. For all examined points of the engine run, the volumetric heat release rate diagrams, cylinder pressure, and temperature illustrate changes that resulted from the tested fueling options. Additionally, engine thermal efficiency and emissions are presented. Because of potential application, the tests were confined to one engine speed (n = 1500 rpm). The research confirmed the possibility of efficiently applying raw *Camelina sativa* oil as an HRF for DF engines and ethanol (LRF) under high-load conditions.

History

Received: 04 Dec 2023
Revised: 17 May 2024
Accepted: 18 Jul 2024
e-Available: 06 Aug 2024

Keywords

Biofuels, Ethanol, *Camelina sativa*, Premixed dual-fuel combustion

Citation

Pawlak, G., Skrzek, T., Kosiuczenko, K. Płochocki, P. et al., "Premixed Dual-Fuel Combustion of *Camelina sativa* Oil and Ethanol," *SAE Int. J. Engines* 17(8):995-1015, 2024, doi:10.4271/03-18-01-0001.

ISSN: 1946-3936
e-ISSN: 1946-3944

This article is part of a focus issue on Fossil Free Alternate Fuel Technology for IC Engines: Part 2.

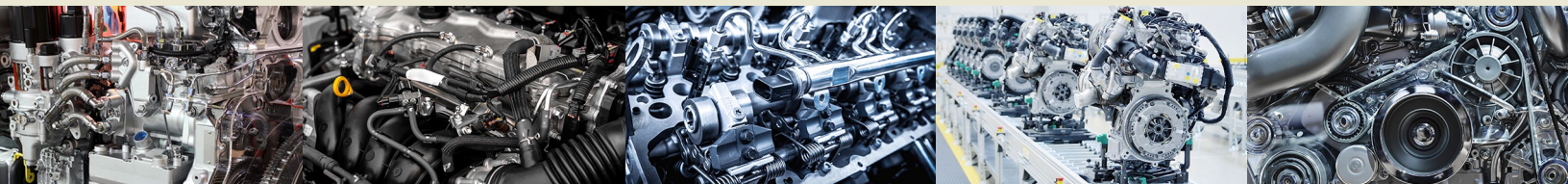

1. Introduction

Looking back, the changes in the energy sector took decades [1]. Although hydrogen seems to be the fuel of the future, there is still no single scenario for the development of the energy production market, especially in Europe, where the transition to renewable energy sources must reach such a rapid pace as proposed in the "Fit to 55" strategy [2]. Despite many disadvantages, an internal combustion (IC) engine adapted to renewable fuels is still a technological alternative, allowing for effective energy generation, especially in cogeneration systems, including heat energy production. One of the trends in research in IC engines is to reach a CO_2 net-zero operation. This idea can be implemented by applying non-fossil fuels like biofuels, synthetic fuels, or hydrogen.

Dual-fuel (DF) engines utilize the diesel process to burn lean mixtures of low-reactive fuel, including biofuels (e.g., ethanol or biogas) ignited by a fuel of high reactivity (e.g., biodiesel or raw vegetable oil) [3, 4, 5]. This technology, utilizing renewable fuels, could be an option for "green energy" production [6], especially fuels produced near power installations using the least energy-intensive production process possible. Still, it requires adaptation of the engine, including an additional fuel system and its adjustment, to realize the controlled combustion process of specific fuels [7, 8, 9].

In their neat form, many vegetable oils have been tested in CI diesel engines. The application of chosen straight oils to study the effect on performance and emission characteristics of older and new generation CI engines was presented in [10, 11]. Studies on raw *Camelina sativa* (CS) oil combustion were described in [12].

High kinematic viscosity and bigger than diesel oil density of raw vegetable oils may lead to incomplete combustion of such fuel and higher CO and hydrocarbon (THC) emissions as well as to form deposits on engine elements, especially in low temperatures (this could be improved by using suitable pour-point depressants or by blending with diesel oil or kerosene-type fuel, e.g., JP-8 [13]).

Physical parameters like droplet temperature, gas phase temperature, ambient gas pressure, and droplet burning velocity influence the ignition delay and the combustion process in CI engines. Vegetable oils are much more reactive to oxygen, so preheating accelerates the oxidation reaction, partially diminishing the role of phenomena that delay the process of creating a flammable mixture. Preheating raw vegetable oil could significantly contribute to the control of ignition and combustion processes [14].

The high-pressure circuit in a common rail system raises the fuel's temperature, contributing to the modification of fuel properties, including kinematic viscosity reduction. The drop of oil viscosity increases the possibility of obtaining a fuel droplet diameter spectrum in the engine cylinder, allowing for their rapid evaporation and the formation of a combustible mixture.

Despite the transesterification of vegetable oils and their additional treatment to provide high-quality fuel, skilled labor, equipment, energy, and chemicals are required. It is also a time-consuming and expensive process [15].

Using raw vegetable oil as fuel in local energy production installations may benefit the environment. The authors of [16] described in detail the greenhouse gas emissions from the production of rape biodiesel (FAME) in a few scenarios of its production. The increase in the calculated gCO_2 equivalent per MJ of refined rapeseed oil due to esterification was 12.7% up to 31% in comparison with raw vegetable oil, depending on the production scenario. The calculation included plantation, oil mill, refinery, transport (to port), and esterification. The emission from the transport of the fuel was calculated at 2 gCO_2 eq. per MJ.

Raw CS oil has a high potential for bio-energy production when searching for CO_2-neutral energy sources [17]. One of the key issues is the ability of the plant to adapt to many different environmental conditions. The heavy clay and organic soils are the only limitations of CS cultivation [18]. Another advantage is the short growing season (85–100 days) with a yearly yield of 2600 kg oilseed per hectare (wet weight) on good soil [19]. The oil (30%–43%) is obtained by cold pressing, which is a simple and proven technology [20, 21]. The low energy consumption of the crushing process of seeds (0.165 kWh/L) [22] is closely related to minimizing carbon emissions. CS use as a fuel would benefit the economy and agriculture. Increasing cultivation may be a way to develop large areas of wasteland. Its more extensive production would reduce its relatively high and highly diversified price.

Ethanol can be made from wheat, rye, corn, and other grains, as well as potatoes and sugarcane. It can also be produced from grass and other natural non-food biomass such as cellulosic raw materials, including wood residues or waste [23, 24, 25, 26]. In this case, the release of sugars into ethanol is more complicated, but these processes are constantly being studied and developed. In 2021, the production of ethyl alcohol in the European Union was estimated at approximately 4 million tons (about 5 billion liters) and is still on a similar level [27]. The average ethanol import price in the European Union amounted to $1076/ton ($0.85/L) [28]. The total potential of bioethanol production from crop residues and wasted crops is about 16 times bigger than its current global production [29]. The latest technologies, like electro-organic synthesis [30, 31], allow us to look at ethanol differently. CO_2 is treated as a carbon source, and ethanol enables energy storage, distribution, and consumption on demand. If the plan to replace IC engines with electric propulsion in new vehicles gains momentum, the large amounts of ethanol produced, which is currently an additive to petrol, can be used for energy production. Despite many

arguments for the broader use of this fuel, the production of carbon dioxide from ethanol installations [32] and water demand in ethanol production should also be considered [33]. The production of 1 kg of ethanol demands 34.5 MJ of heat [34]. There is room to reduce the energy consumption of the process. The energy production facility's design may include using the engine waste heat. Also, CS sawdust [35] could be used to produce heat in such an installation. The heating value of CS gray strove is 15.2 MJ/kg. Also, the pomace can be the source of the heat energy. Its heating value is 22 MJ/kg [36].

Both fuels, CS oil and ethanol, can be produced near an energy production installation, contributing to the confining of the environmental impact of fuel transportation. Summing up, there are many environmental and technical reasons for the proposed way of energy production:

1. The potential to reduce CO_2 emissions,
2. The short track "from well to wheel" (exactly: "from field to plug"),
3. Modification of CI engine required to fuel it with renewable liquid fuels are more limited than those needed for fueling with hydrogen or biogas [37],
4. The broader interest of an easy-to-introduce crop (CS) to agriculture [38],
5. Potentially good access to fuels, especially in the agriculture industry,
6. Flexibility (the engine can be fueled with CS only or with both fuels in various proportions),
7. Utilization of energy stored in ethanol produced on a big scale utilizing new technologies in the future,
8. Easy storage of liquid fuels is less demanding than, e.g., biogas storage installation [39].

CI engines used in power generators are currently equipped with a common rail system. Such a system enables the realization of the DF partially premixed combustion. The HRF/LRF proportions, the injection timing of the direct-injected HRF, and exhaust gas recirculation (EGR) can be employed to modify and control the combustion phasing [40].

In a previous study [41], the authors showed that raw CS oil, despite different properties than diesel oil, can be burned efficiently in a CI engine equipped with common rail system. The main novel aspect of this work is presenting the possibility of its application as an HRF for DF engines together with ethanol (LRF) under high-load conditions (about 75% of the maximum load of the engine fueled with diesel oil). The work aims to test and describe the premixed DF combustion (PDFC) of raw CS oil (HRF) and ethanol (LRF) based on experimental results. In particular, the possibility of controlling the combustion process of a DF mixture using the proposed injection strategy of CS.

2. The Control of DF Combustion Process

The DF combustion demands proper organization. The simple injection strategy called conventional dual fueling (CDF) means a late injection of the HRF into the combustion chamber where the LRF/air mixture was created after the port injection of LRF. It results in delayed ignition of the premixed lean mixture due to premixed lean autoignition, which can occur at many locations in the combustion chamber. HRF can be injected much earlier than required by the CDF strategy. Early mixing of the HRF with the LRF allows the HRF to mix with the air. It eliminates areas of rich and near-stoichiometric mixing where soot and NO_x are produced, contributing to NO_x [42] and PM emissions reduction. The strategy is called reactivity-controlled compression ignition (RCCI) [43]. Combining the early HRF injection of RCCI and the late HRF injection of conventional fueling leads to a hybrid combustion mode referred to as PDFC [44]. PDFC enables high engine thermal efficiency, NO_x, and soot emissions similar to RCCI, but without its high cylinder pressure peak and high rates of cylinder pressure rise [45, 46].

The combustion process of a DF mixture also depends on the engine design features, such as the compression ratio [47] and the combustion chamber's shape [48]. The impact of the compression ratio and injection parameters on the combustion characteristics and emissions in DF operation for fueling with methane and diesel oil is presented in [49]. In particular, a compression ratio of 15.5 reduced methane unburnt and combustion noise. Still, the mixture composition and fueling process parameters are crucial. The following parameters affect DF combustion:

1. Division and injection timing of a pilot dose (usually, a single pilot dose injection is applied, but a common rail system allows the experimentation with multi-injection strategies),
2. The injection pressure of a pilot dose,
3. Amount of HRF injected per cycle,
4. Amount of LRF supplied per cycle,
5. Amount of intake air, its temperature and pressure,
6. Rate and temperature of EGR.

The total excess air coefficient for dual-fueling (λ_{DF}) and substitution rate (E_{eth}) describes the DF mixture composition. The total excess air coefficient for dual-fueling (λ_{DF}) is defined as:

$$\lambda_{DF} = \frac{m_A}{L_{LR} \cdot m_{LR} + L_{HR} \cdot m_{HR}} \quad \text{Eq. (1)}$$

where
m_A is the mass of the air [kg]
m_{LR} is the mass of LRF (ethanol) [kg]
m_{HR} is the mass of HRF (CS) [kg]
L_{LR} is the theoretical air required for complete combustion of 1 kg of LRF (ethanol) [kg/kg]
L_{HR} is the theoretical air required for the complete combustion of 1 kg of HRF (CS) [kg/kg]

The portion of total fuel energy provided by LRF (in this case ethanol) to the combustion chamber is defined as the substitution rate (E_{eth}):

$$E_{eth} = \frac{LHV_{eth} \cdot m_{eth}}{LHV_{cs} \cdot m_{cs} + LHV_{eth} \cdot m_{eth}} \cdot 100\% \qquad \text{Eq. (2)}$$

where
LHV_{eth} is the lower calorific value of ethanol [MJ/kg]
m_{eth} is the mass of ethanol [kg]
LHV_{cs} is the lower calorific value of CS [MJ/kg]
m_{cs} is the mass of CS [kg]

The stability of the DF combustion process deteriorates due to the lack of an ignition source and locally varied in-cylinder mixture composition. When operating at the part load, DF engines can suffer from the excessive incomplete combustion of the primary fuel (LRF), resulting in increased unburned fuel emissions. Due to the high compression ratio of CI engines, the substitution rate at high loads is often limited by engine knock and pre-ignition [50]. The knocking combustion usually occurs when a portion of the unburned gases in front of the flame front spontaneously ignites. They may self-ignite at one or more points. Knock causes high-amplitude local pressure waves and generates high-frequency pressure oscillations [51]. Division of the HRF dose and optimizing the injection timing reduce the high peak pressures that generally act as a limiting factor for DF engine operation [52].

For different LRF fuels, the knock appearing after their ignition is a unique phenomenon. In the case of fueling with natural gas and diesel oil, the detonation of the mixtures was observed in regions between the individual diesel spray jets. The calculation results presented in [50] gave information about the autoignition and the knock combustion of ethanol/gasoline blend (E85) ignited by a single dose of diesel oil. At a high load, the most severe knock and the origin of autoignition always occur far away from where the diesel spray flame is first generated. For 50% and 70% of the substitution rate, the knock appeared at the center of the combustion chamber due to the higher pressure wave, relatively richer E85 mixture, and longer distances of flame propagation. The two-stage injection strategies with a small amount of diesel pilot injection ahead of the main injection lead to a lower pressure rise rate and a reduced propagation distance, contributing to the attenuation of knock intensity for a higher E85 percentage in the DF mixture. The injection strategy examined for natural gas and diesel oil described in [45] decreased methane emissions and improved engine efficiency while maintaining low NO_x and soot levels. In this case, PDFC utilized an early diesel injection to adjust the flammability of the premixed charge, promoting a more uniform burning of methane. The strategy was efficient at medium loads. At lower loads, the benefits of PDFC are reduced due to higher in-cylinder total excess air coefficient (λ_{DF}) and too low temperature and pressure to promote autoignition. The early injected diesel oil mass was limited to confine cylinder pressure rise at a higher load.

The phenomena related to the dual fueling of CI engines were taken into account in the experiment presented in the article. The literature does not describe how specific properties of the fuels used in the experiment affect their self-ignition and DF combustion.

3. Raw CS Oil and Ethanol for Dual Fueling of CI Engine

The comparison of the combustion process for the same injection strategy applied for CS and diesel oil showed differences resulting from their different physical and chemical properties [41]. The experiment described there showed the benefits of the common rail system application for injecting vegetable oil connected with the rising injected fuel temperature and possible modification of the heat release process by adjusting the injection strategy. The fuel injected through the common rail system is heated up to 70°C, and as a result, its viscosity is reduced. The measured kinematic viscosity of CS used in the experiment at the temperature of 70°C was 13 mm^2/s. It dropped by 55% compared with the viscosity measured at 40°C (29 mm^2/s) [41]. The property favoring the use of CS is relatively low sulfur content (about 13 ppm) comparable to the 10 ppm required for diesel fuel (Table 1).

TABLE 1 Raw *Camelina sativa* oil, ethanol, and diesel oil properties [58, 59, 60, 61].

Properties	Unit	*Camelina sativa*	Ethanol	Diesel oil
Low heating value	MJ/kg	38.7	25.7	43.2
Cetane number	-	42.3	8	55.0
Liquid density at 15°C	kg/m^3	923	789	831
Kinematic viscosity at 40°C	mm^2/s	29.0	1.36	2.35
Sulfur content	mg/kg	13.8	-	10.0
Water content	mg/kg	720	4.0	43.8
Ash	kg/kg	0.003	-	0.01
Flash point	°C	>220	17	55

Data taken from Refs. [50, 51, 52, 53].

Nevertheless, the sulfur content in fuel should be reduced due to its harmful impact on people and the environment [53]. Higher shares of ethanol (with higher degrees of substitution) in the DF mixture contribute to reducing sulfur compound emissions by limiting the amount of CS, which in this case is their source.

The application of ethanol as a fuel for CI engines is a challenge. The compression ratio of a serial-produced ethanol CI engine is 28, and ethanol is mixed with an "ignition improver," enabling its controlled ignition. In this case, the engine's performance, including thermal efficiency, is comparable to conventional CI engine parameters [54]. Another possible ethanol application in CI engines is presented in [55]. The test of fuel blends consisting of diesel, gasoline, and ethanol (Diesehol) showed an overall improvement in engine efficiency when running on fuels with 30% ethanol content. Results also showed a higher amount of CO and THC since the combustion process was degraded due to the cooling effect of alcohol.

Other shortcomings of ethanol are:

1. Poor lubrication properties resulting from low viscosity and degradation of lubricating oil properties,
2. Corrosion and chemical degradation of engine materials.

Ethanol usage for DF operation demands limited engine modification, allowing its co-burning with an HRF [56]. The DF approach permits flexible control of the premixed combustion, especially at medium and high-load operations and, as a result, it is possible to decrease NO_x and soot emissions simultaneously while improving the thermal efficiency [57].

Due to the high reactivity, CS can be used as a fuel to ignite a DF mixture. In such an application, evaporating alcohol cools the combustion chamber space, which may reduce the excessive formation of sediment caused by thermal polymerization at the tip of the nozzles. It can benefit the reliability of dual-fuel engines fueled with vegetable oils. Their higher kinematic viscosity contributes to forming such deposits. The properties of CS and ethanol are compared with those of diesel oil and presented in Table 1.

4. Results and Discussion

The experiment was carried out on an AVL 5402 experimental CI engine (Table 2) with a typical compression ratio of 17, equipped with a common rail system for engine speed n = 1500 rpm, yielding generator frequency. During engine tests, cylinder pressure diagrams from 100 cycles were registered, and the parameters describing the combustion process were calculated using AVL software (AVL Concerto ver. 4.4b). For the exhaust gas analysis, AVL SESAM i60 FT analyzer was used.

TABLE 2 Engine characteristics.

Model	AVL 5402
Type	Four-stroke, naturally aspirated, direct injection
Displacement [cm^3]	511
Number of cylinder	1
Bore/stroke [mm]	85.01/90.00
Compression ratio	17
Maximum effective power without supercharging for diesel oil fueling [kW]	6
Fuel system	Common rail
Maximum power [kW]	ca. 16
Maximum speed [rpm]	4200
Inlet valve open/close [CA deg]	346/586.5
Exhaust valve open/close [CA deg]	128.5/376.5
Valve overlap [CA deg]	80
Nozzle type	DLLA 162 P 2160

Data taken from Ref. [62]. © Military Institute of Armored and Automotive Technology

Information about uncertainty for key measurement equipment is included in [63]. Percentage equipment variation (%EV), which is a measure of the repeatability of the measurement experiment calculated for the AVL system used in the test is %EV = 0.4% (the measurement system is considered appropriate for the specific task if its %EV is below 10%). The maximum error of the pressure measurement in the combustion chamber is $\Delta p = \pm 0.4\%$. The fuel consumption measurement accuracy (Ra) for the Bronkhorst Cori-Flow flowmeter used in the experiment was calculated using the formula Ra = ±(0.2% reading + 8 g/h). Maximum error of fuel consumption was $\Delta G_h = \pm 0.77\%$. The maximum error of engine speed measurement was $\Delta n = \pm 10$ rpm. The maximum error for λ measurement (Lambda Meter LA4) was $\Delta\lambda = \pm 1.0\%$. The calibration process of AVL SESAM i60F.T. analyzer and the rest of the measurement equipment was carried out following the manufacturer's recommendations. Figure 1 shows a general layout of the test stand.

The experiment was divided into three parts. The first one included verification of the injection strategy, which allowed the realization of PDFC. The study included the test of PDFC of raw *CS* oil (HRF) and ethanol (LRF) for various substitution rates (E_{eth} = 21%, 49%, and 80%) to show the main differences in the combustion process for a low, middle, and high portion of total fuel energy provided by ethanol to the engine cylinder (Section 4.1).

Because engine knock limits DF engine operation, the injection timing of CS and EGR influence the DF combustion process for middle (Section 4.2) and high (Section 4.3) substitution rates was tested. The amount of both fuels provided to the engine cylinder per one cycle was determined by the assumption of constant total excess air coefficient λ_{DF} and the substitution rate E_{eth}.

The process was examined for constant total excess air coefficient λ_{DF} = 1.3, typical for highly loaded CI engines.

FIGURE 1 General layout of the test stand. 1. Engine, 2. *Camelina sativa* oil tank, 3. Electric fuel pump, 4. Fuel filter, 5. High-pressure fuel pump, 6. Rail, 7. Fuel pressure sensor, 8. Injector, 9. Common rail supply system controller, 10. Crankshaft speed sensor, 11. EGR cooler, 12. EGR valve, 13. Exhaust throttle, 14. Ethanol controller supply system, 15. Ethanol injector, 16. Ethanol tank.

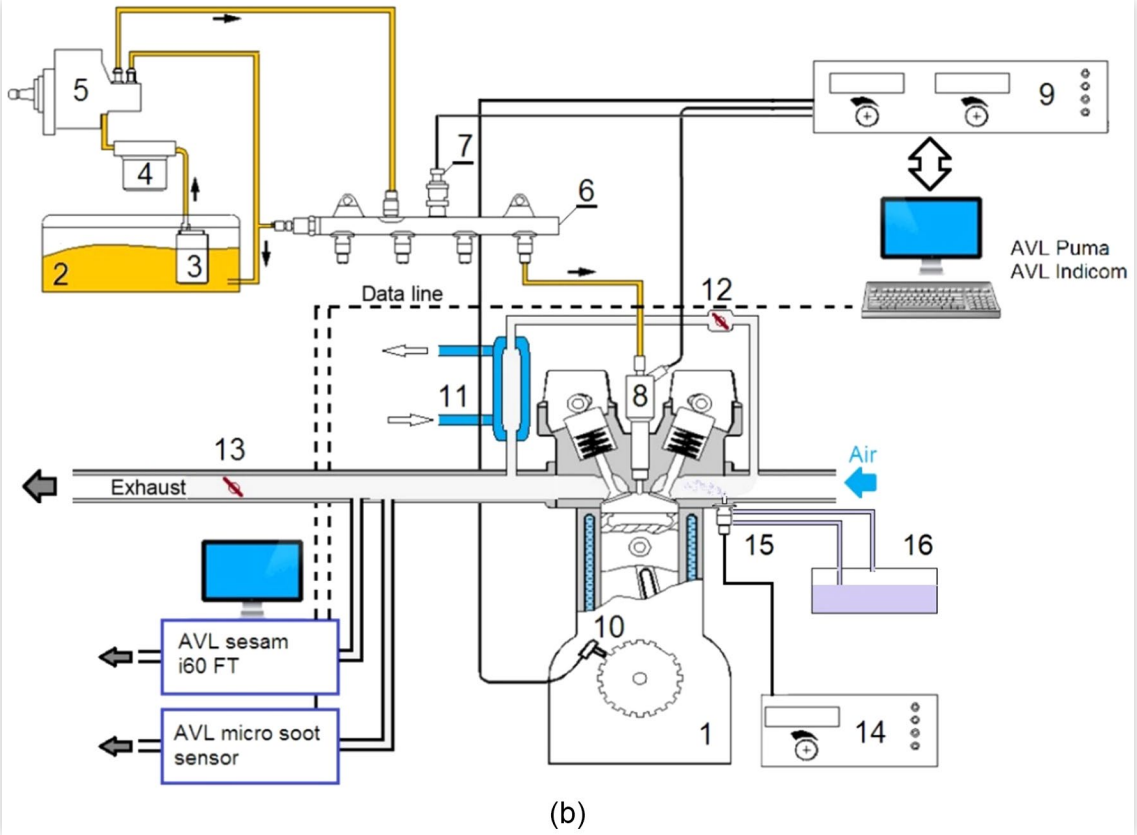

The addition of EGR, with the same dose of both fuels, caused a decrease in λ_{DF} to 1.1 (Sections 4.2 and 4.3).

In order to illustrate the injection process, the voltage signal from the common rail injector has been registered and shown in the diagrams of volumetric heat release rate (VHRR) and cylinder pressure (p) presented in the article. CS injection pressure was p_{in} = 65 MPa. Ethanol was injected into the engine inlet channel after opening the inlet valve. Its injection pressure was set at p_{eth} = 0.3 MPa.

4.1. DF Combustion for Different Substitution Rates

The first part of the experiment showed characteristic phenomena influencing the DF combustion at various substitution rates (E_{eth}). The experiment on PDFC was preceded by fueling the engine with CS only (E_{eth} = 0%) to find an optimal injection strategy for λ = 1.3. Its total dose was divided into a preliminary dose selected from the initial test (2.4 mg/cycle) and a main dose. The start of injection of the preliminary dose (SOI_1) was constant (16 deg BTDC). The mass of the main dose and its start of injection (SOI_2) were adjusted to the substitution rate (E_{eth}).

The results obtained for different substitution rates (E_{eth}) were compared to those obtained for CS only (E_{eth} = 0%) and are presented in Figures 2 and 3.

The changes in substitution rate significantly modified the DF combustion process. From E_{eth} = 0% to E_{eth} = 80% the process has evolved from partially premixed compression ignition combustion (PPCI), achieved by early and late CS direct injection, to PDFC. The injection of the preliminary dose creates a stratified lean premixed DF mixture in the engine cylinder. Its lean premixed autoignition (LPA) caused the heat release and heated up the chamber before the later main dose injection (SOI_2). The heat reduced the ignition delay of the rich premixed mixture from the late injection of the main dose of CS. The phenomenon is visible in the VHRR diagram at E_{eth} = 0% (CS only) and E_{eth} = 21% [Figure 2(a)].

For the middle and high E_{eth}, the SOI_2 is delayed to confine dp/dα. In the case of E_{eth} = 49%, the premixed combustion started at the beginning of the main dose of CS injection. Consequently, the volumetric heat release process had two phases [Figure 2(a)]. The stratified LPA and combustion were observed in the first phase. In the second phase,

FIGURE 2 (a) Volumetric heat release rate—VHRR, (b) cylinder pressure—p with a signal from CS injector, and (c) in-cylinder temperature—T for DF mixture without EGR at different substitution rates—E_{eth} (averaged diagram from data for 100 consecutive cycles).

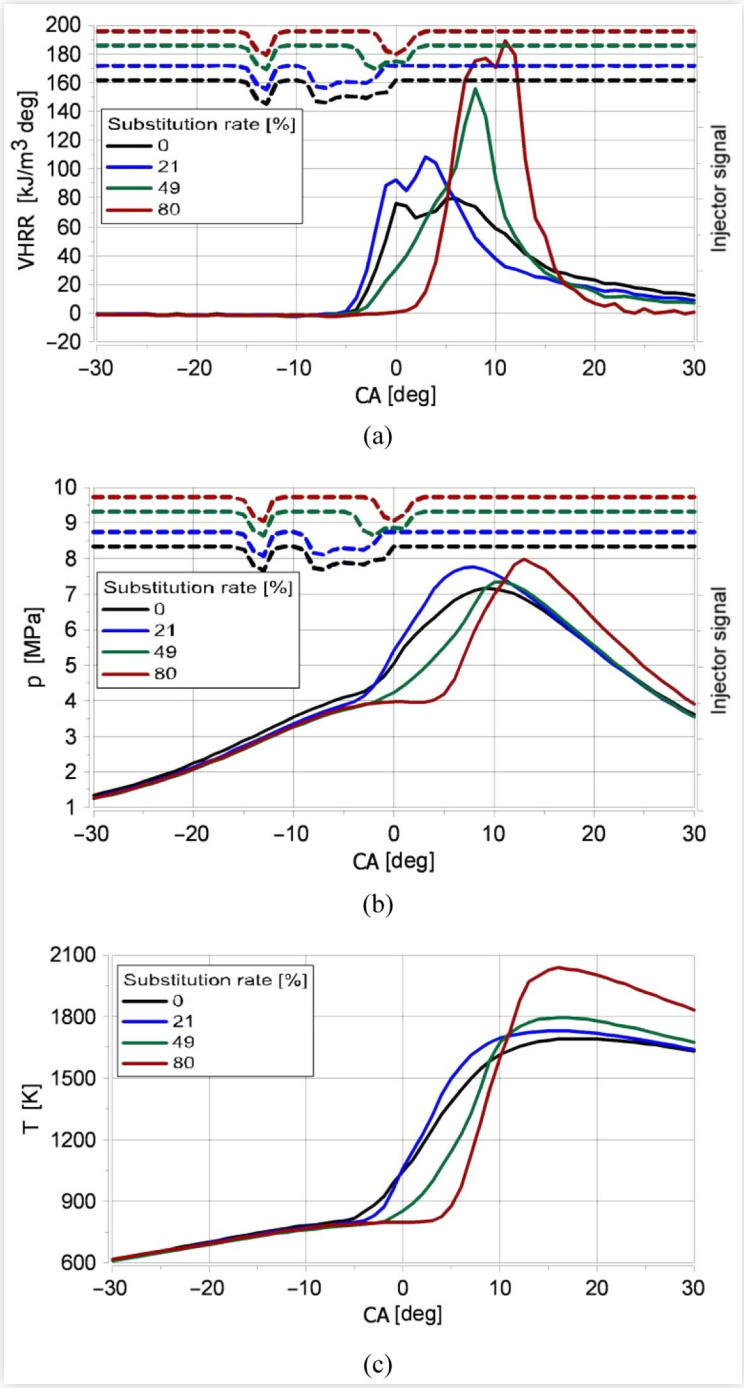

quasi-homogeneous combustion started with no rapid VHRR growth. The stratified LPA and premixed combustion phase are stretched out, and the autoignition of the quasi-homogeneous mixture follows it. Because of the relatively low ethanol content in the quasi-homogeneous mixture, the peak in the VHHR diagram is small [Figure 2(a)]. The stratified and quasi-homogeneous combustion phases are not separated, so there were no sharp changes in the reactivity gradient in the combustion chamber.

For E_{eth} = 80%, the late autoignition caused by the late injection of CS main dose occurred. Despite the late injection of the main dose of CS, it was possible to burn 50% of the fuel (MFB_{50}) as fast as CS was burnt without ethanol [E_{eth} = 0%, Figure 3(c)]. The cylinder pressure rise rate was acceptable

(dp/dφ = 7 bar/deg) in this case [Figure 3(d)]. As a result, the maximum cylinder pressure was shifted but wasn't too high [Figure 2(b)]. It was noted that CS efficiently ignited the DF mixture, so the engine cycles were repetitive. For all examined substitution rates, cycle-by-cycle variations of indicated mean effective pressure (CV_{IMEP}) remained acceptable [Figure 3(f)]. Still, more ethanol in the mixture caused a drop in engine thermal efficiency (η_{th}) [Figure 3(e)]. Due to indirect ethanol injection, a part of the air/fuel mixture was escaping to the exhaust pipe [Figure 3(j)]. Also, the ethanol evaporation process consumed some energy. It is visible in the in-cylinder temperature diagram [Figure 2(c)]. The temperature inside the combustion chamber for E_{eth} = 80% was nearly constant between 3 deg BTDC and 3 deg after TDC [Figure 2(c)]. The retarded combustion, which took place in a larger volume above the piston, led to heat losses through the larger area of

FIGURE 3 Measured and calculated engine parameters and emissions for DF mixture without EGR at different substitution rates (E_{eth}): (a) Q_c, (b) BMEP, (c) MFB50, (d) dp/dα, (e) η_{th}, (f) COV_{IMEP}, (g) t_{exh}, the volumetric share of (h) H_2O, (i) CO, (j) THC, (k) NO_x in exhaust gases, (l) PM concentration in exhaust gases.

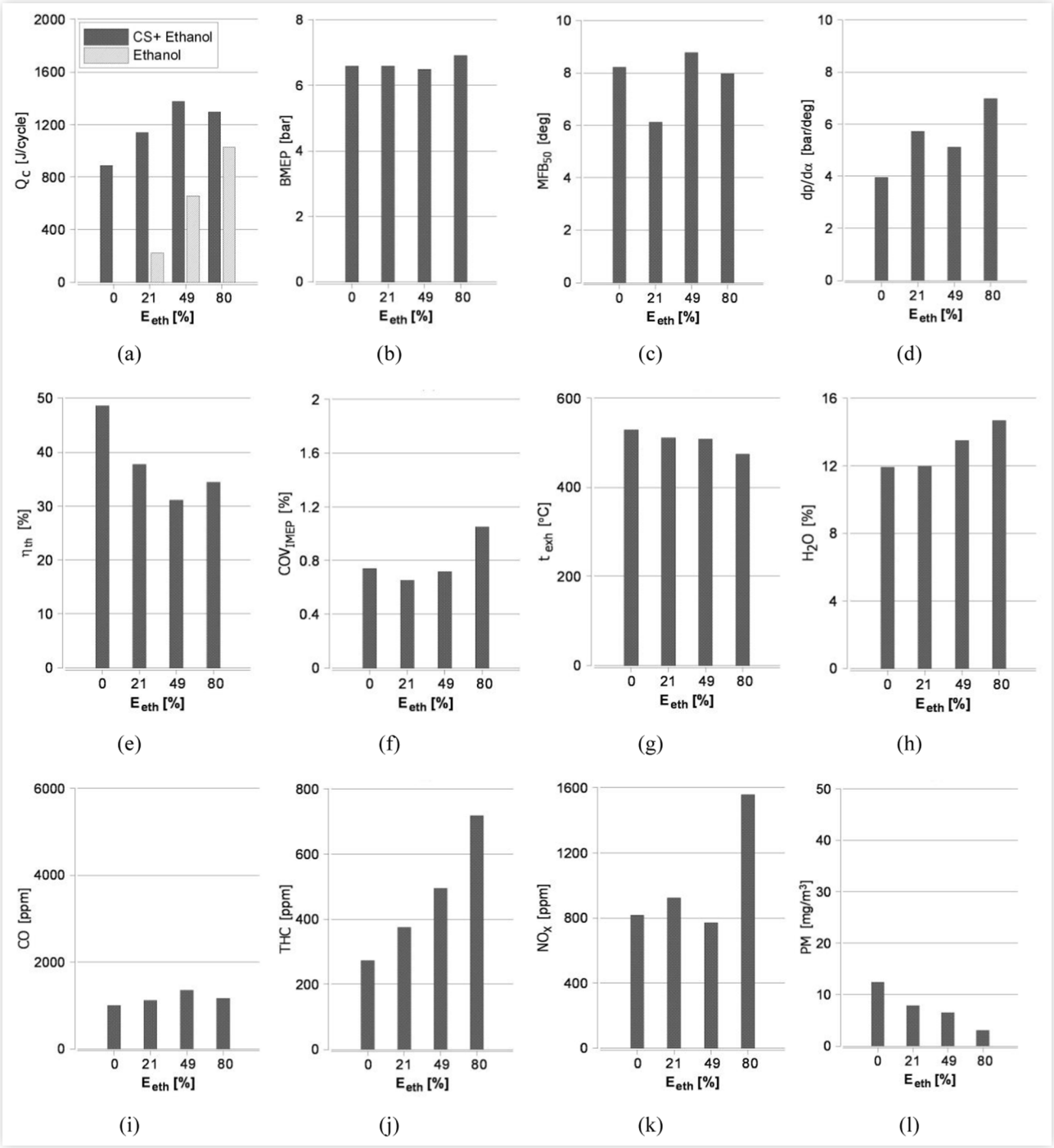

the cylinder wall surrounding the burning mixture. More ethanol in the DF mixture resulted in more water vapor in the exhaust gases [Figure 3(h)]. The evaporation of water in the combustion chamber consumed some heat, decreasing the BMEP [Figure 3(a)], and reducing engine thermal efficiency (η_{th}). However, some heat in the water vapor can be recuperated outside the engine in a cogeneration unit. It was observed that exhaust gas temperature (t_{exh}) was lower at high E_{eth} [Figure 3(g)]. It can be explained by the higher volumetric share of water vapor (high specific heat capacity) in exhaust gases.

The high E_{eth} positively affected PM emissions. It could be reduced to 1–3 mg/m^3 compared to 8–13 mg/m^3 for fueling with CS only [Figure 3(l)]. The incomplete combustion of the DF mixture for high E_{eth} resulted in high CO [Figure 3(i)] and THC [Figure 3(j)] emissions. In Figure 4 some characteristic parameters of the injection of CS and combustion process of DF mixture for different substitution rates (E_{eth}) are compared.

The in-cylinder temperature diagrams [Figure 2(c)] show the convergence between in-cylinder temperature and NO_x emissions [Figure 3(k)]. The high in-cylinder temperature (maximum in-cylinder temperature higher than 2000 K for E_{eth} = 80%) resulted in a twice higher share of NO_x in the exhaust gases than for lower E_{eth}. NO_x formation mainly depends on the temperature of the burnt gas, the residence time of the burnt gas, a high temperature, and the amount of excess oxygen and turbulence [64]. The formation rate of thermal NO is slow below 1800 K and than increases exponentially. For DF mixture rich in ethanol (E_{eth} = 80%) after big ignition delay the combustion lasts more than two times shorter (Figure 4) than for small (E_{eth} = 21%) and medium (E_{eth} = 49%) share of ethanol in the DF mixture. It means that a similar amount of heat that is released during combustion of all analyzed DF mixtures [Figure 3(e)] is released in much shorter time in this case. The result is high cylinder temperature and as a consequence high NOx emission. The mechanism of autoignition and combustion of DF mixture is really complex. Chemical kinetic analyses employing a detailed mechanism to gain insights into the chemistry of the DF mixture could provide a detailed explanation of its autoignition, combustion, and, as a consequence, explain emissions in details. Such a study is presented in [65] where the autoignition of methane/diesel mixtures with varying diesel contents (30%, 50%, and 70%) over an extensive range of temperature, pressure, and equivalence ratio is presented.

4.2. DF Combustion for a Middle Substitution Rate

In the following test, the DF combustion at a middle substitution rate (E_{eth} = 49%) was tested. Like in Section 4.1, CS dose was divided into a preliminary dose (2.4 mg/cycle) and a main dose. The start of injection of the preliminary dose of CS (SOI_1) remained constant (16 deg BTDC).

To check the influence of EGR on the combustion process of the DF mixture and to show how the injection timing affects the process, the mixture with EGR was examined for different SOI_2, and the results were compared to one point of engine run without EGR (SOI_2 = 5 deg BTDC) described in Section 4.1. The cooled EGR (24% rate) at a temperature of 25°C was applied. The EGR application limited the air delivered to the engine's combustion chamber in one cycle. As a result, the total excess air coefficient was reduced to λ_{DF} = 1.1. The results of this part of the experiment are presented in Figures 5 and 6.

FIGURE 4 The comparison of some characteristic parameters of the injection of CS and the combustion process of DF mixture at different substitution rates—E_{eth} (yellow lines describe the injection, but red lines refer to the combustion).

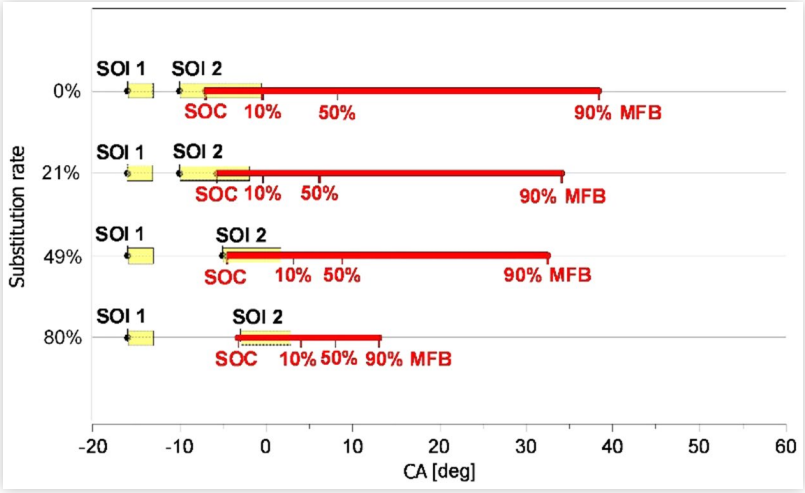

FIGURE 5 (a) Volumetric heat release rate—VHRR, (b) cylinder pressure—p, and (c) in-cylinder temperature—T diagrams with a signal from CS injector for the various SOI_2, E_{eth} = 49%, EGR (for comparison: E_{eth} = 49%, without EGR and SOI_2 = 5 deg BTDC), (averaged data for 100 consecutive cycles).

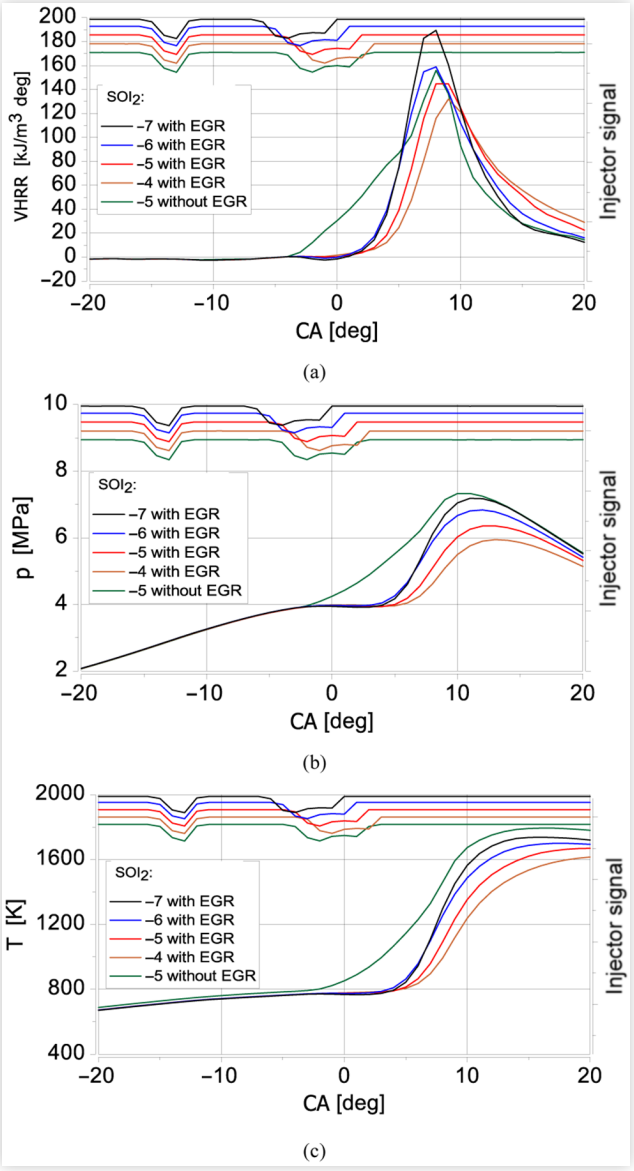

The EGR changed the combustion course significantly. The autoignition was delayed, and the quasi-homogeneous combustion was observed. The later SOI_2 for medium E_{eth} caused a slight drop in BMEP [Figure 6(b)], and the rise of COV_{IMEP} [Figure 6(f)]. The modification of the combustion process caused by EGR, in this case, raised emissions of CO [Figure 6(i)], THC [Figure 6(j)], and PM [Figure 6(l)]. Still, NO_x dropped significantly [Figure 6(k)] because of the drop in in-cylinder temperature [Figure 5(c)]. The temperature of exhaust gases rose slightly, and H_2O was similar to the DF mixture combustion without EGR. The characteristic points of the injection of CS and combustion process for E_{eth} = 49% are presented in Figure 7.

The combustion started later for the earlier injection of the main dose of CS, but 90% of the fuel was burned approximately 40 deg after TDC for all examined points with EGR. It affected the cylinder pressure, especially the CA deg for maximum cylinder pressure, which hasn't changed significantly [Figure 5(b)], but dp/dα dropped for later SOI_2 [Figure 6(d)]. No significant changes in η_{th} were observed [Figure 6(e)].

4.3. DF Combustion for a High Substitution Rate

The next part of the experiment shows the influence of injection timing of the main dose of CS (SOI_2) on DF mixture combustion at a high substitution rate (E_{eth} = 80%). Parameters of the preliminary dose of CS remained unchanged in this part of the test (2.4 mg/cycle, SOI_1 = 16 deg BTDC). The SOI_2 was changed up to the limit, resulting from the appearance of the knock. The combustion of DF mixtures without EGR and with cooled EGR were examined, and the results were compared. Figures 8 and 9 illustrate the results at E_{eth} = 80% without EGR. The total excess air coefficient was maintained at λ_{DF} = 1.3.

The change of SOI_2 tested in a wide range for E_{eth} = 80% without EGR enabled the observation of the quasi-homogeneous combustion process of the DF mixture. Results show that a significant advance of CS main dose injection (SOI_2 = 5 deg BTDC) led to earlier MFB_{50} [Figure 9(c)] and an unacceptable high cylinder pressure rise rate (dp/dα) [Figures 8(b) and 9(d)], which induced engine knock (Figure 12). For the rest of the tested SOI_2 values (between 3 deg BTDC up to 3 deg ATDC) the maximum of dp/dα was acceptable. The change of SOI_2 didn't affect Q_c [Figure 9(a)], BMEP [Figure 9(b)], η_{th} [Figure 9(e)], COV_{imep} [Figure 9(f)], also CO [Figure 9(i)]. Also, THC emissions [Figure 9(j)] were similar for all tested values of SOI_2. The rise of in-cylinder temperature [Figure 8(c)] caused high NO_x emissions [Figure 9(k)]. Also, PM [Figure 9(l)] strongly depended on SOI_2. Its change slightly modified exhaust gas temperature [Figure 9(g)] but significantly impacted H_2O volumetric share in exhaust gases [Figure 9(h)], especially for SOI_2 = 5 deg BTDC.

In the next step, a cooled EGR was added (24% EGR rate at a temperature of 25°C). As was mentioned in Section 4.2, the EGR reduced the total excess air coefficient to λ_{DF} = 1.1. The results of this part of the experiment are presented in Figures 10 and 11.

The application of cooled EGR shifted the start of combustion by 3–5 CA deg. However, it didn't significantly modify the VRHR and cylinder pressure shape [Figure 10(a) and (b)]. Still, it resembled the heat release process observed in SI engines. Although most heat was released far from TDC, the process was quick. Generally, it took less time than for the mixture without EGR. In this case, MFB_{90} was less dependent on SOI_2 (Figure 13). The early injection of CS slightly improved engine performance [Figure 11(a)–(c)]. The drop of NO_x emission [Figure 11(k)] resulted from a drop in in-cylinder

FIGURE 6 Measured and calculated engine parameters and emissions for the different SOI_2, E_{eth} = 49%, EGR (for comparison: E_{eth} = 49%, without EGR, SOI_2 = 5 deg BTDC): (a) Q_c, (b) BMEP, (c) MFB_{50}, (d) $dp/d\alpha$, (e) η_{th}, (f) COV_{IMEP}, (g) t_{exh}, the volumetric share of (h) H_2O, (i) CO, (j) THC, (k) NO_x in exhaust gases, (l) PM concentration in exhaust gases.

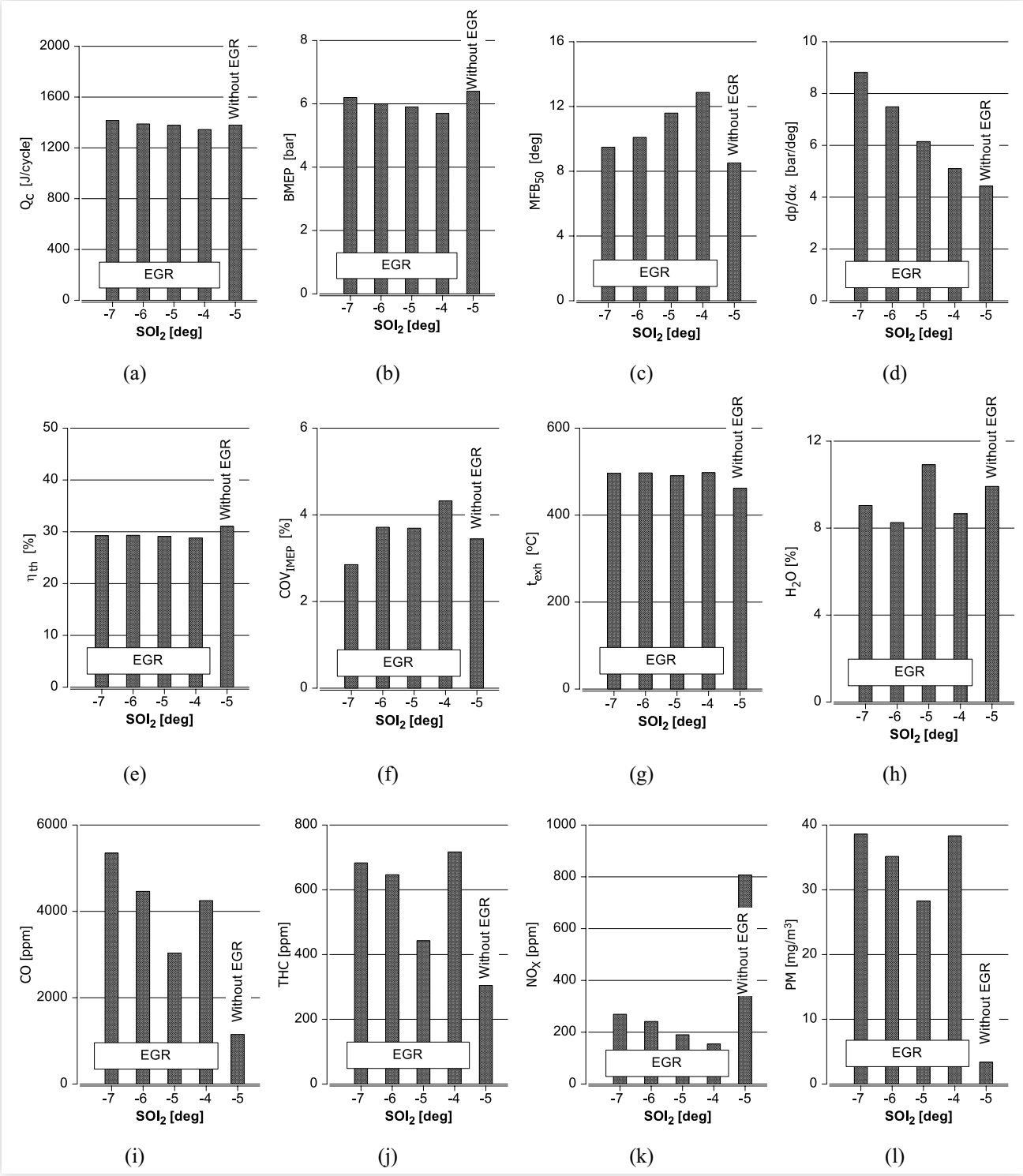

FIGURE 7 The comparison of some characteristic parameters of the injection of CS and the combustion process of DF mixture at E_{eth} = 49% and various SOI_2, EGR (for comparison: E_{eth} = 49%, without EGR, SOI_2 = 5 deg BTDC) (yellow lines describe the injection, but red lines refer to the combustion).

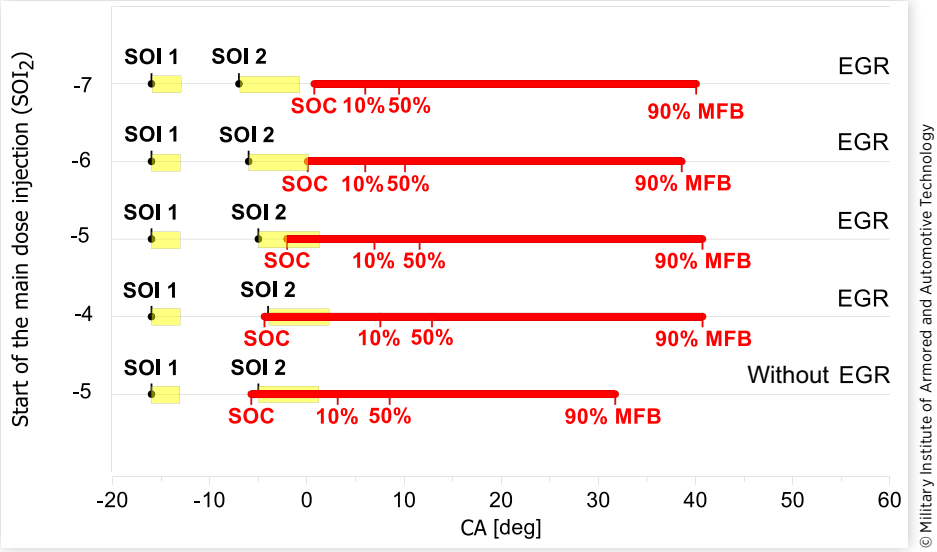

temperature for late SOI_2. Still, PM emission was much higher in this case [Figure 11(l)]. CO [Figure 11(i)] and THC [Figure 11(j)] emissions had their minimum for SOI_2 = 3 deg BTDC. The slightly lower T_{exh} [Figure 11(g)] and the highest H_2O content in exhaust gases [Figure 11(h)] were noted for this case. COV_{IMEP} [Figure 11(f)] was lower, and early MFB_{50} [Figure 11(c)] was observed for more advanced injection, but for SOI_2 = 7 deg BTDC, the beginning of the engine knock was observed [Figures 11(d) and 12].

The comparison of some characteristic parameters of the injection and the combustion process of the DF mixture at E_{eth} = 80% without EGR (λ_{DF} = 1.3) and with EGR (λ_{DF} = 1.1) are presented in Figure 13.

5. Conclusions

One of the research goals was to show differences in the combustion process of DF mixture at different E_{eth}. The experiment showed how to control DF combustion at different E_{eth} to confine the knock and receive the highest possible engine performance.

The DF combustion mechanism strongly depends on both fuels' energetic share. PDFC, which was tested at different E_{eth}, constant engine speed (1500 rpm), and high engine load, can be efficiently realized with a simple fuel injection scheme that utilizes the CS dose's division and the adjustment of the main dose mass and injection timing. CS efficiently ignites the DF mixture even when E_{eth} is high (engine cycles were repetitive).

For all examined points, getting relatively high engine loads was possible even for high substitution rates (E_{eth}). Keeping the cylinder pressure rise rate (dp/dα) under control demanded the regulation of injection timing of the main dose of CS to burn 50% of the fuel (MFB_{50}) before 6–9 deg ATDC, allowing a smooth engine run without the knock.

The experiment showed that the engine fueled with CS only reached the highest thermal efficiency (η_{th}), but the DF combustion process was more efficient at a high substitution rate (E_{eth} = 80%) than at a middle (E_{eth} = 49%.).

The improvement of engine thermal efficiency demands further investigation. The applied EGR contributed to a bigger ignition delay of the DF mixture (E_{eth} = 80%). In the case of the middle substitution rate (E_{eth} = 49%), the recirculated exhaust gases could modify the combustion process in a significant way, retarding the process and reducing the premixed combustion phase. NO_x and PM emissions can be reduced significantly by adequately regulating the injection timing of the CS main dose and EGR application. CO and THC emissions (Figure 3) showed that using the common rail system and the proposed *CS* (HRF) oil injection strategy enabled flexible selection of the ethanol/*CS* proportion in the DF mixture and its proper combustion. The experiment confirmed the benefits of using the common rail system for vegetable oil injection related to increased fuel temperature and decreased density and kinematic viscosity.

FIGURE 8 (a) Volumetric heat release rate—VHRR, (b) cylinder pressure—p, and (c) in-cylinder temperature—T diagrams with a signal from CS injector for various SOI_2, E_{eth} = 80%, without EGR (averaged diagram from data for 100 consecutive cycles).

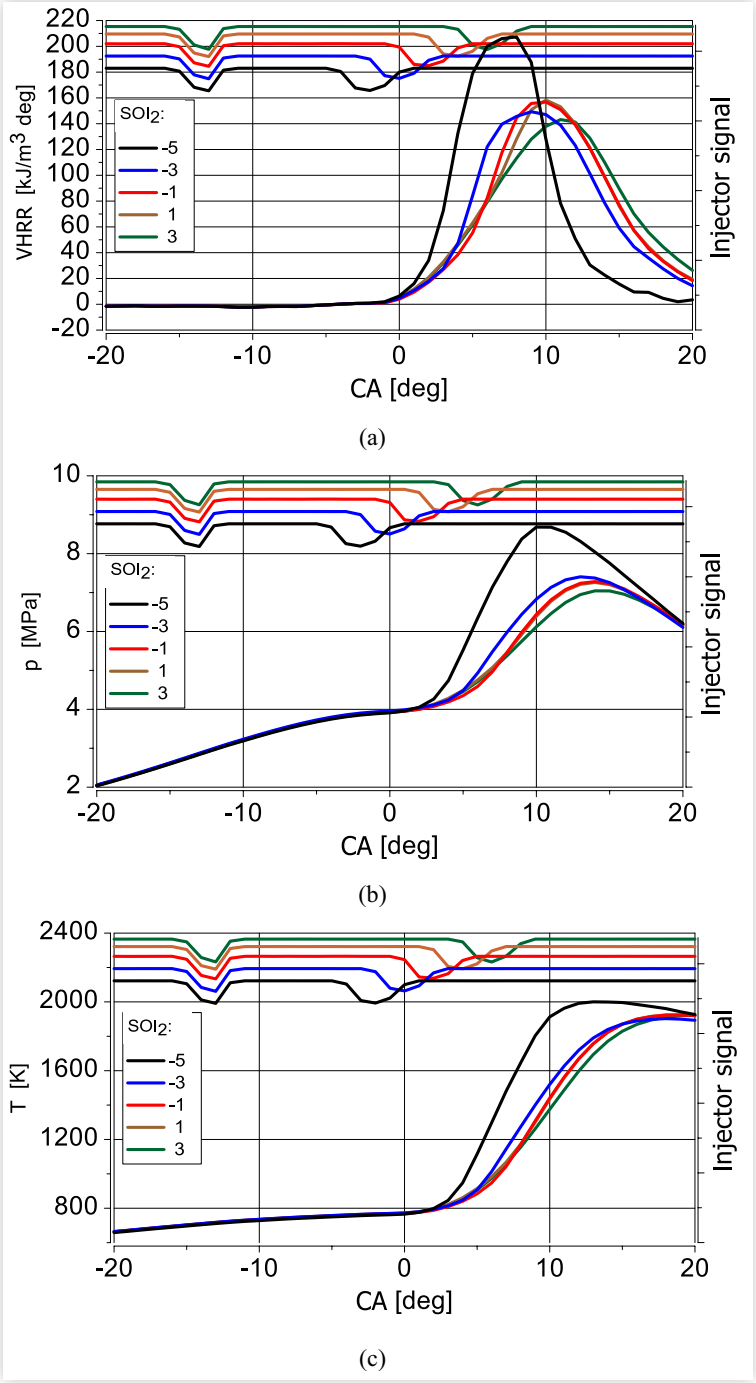

FIGURE 9 Measured and calculated engine parameters and emissions for various SOI_2 for E_{eth} = 80%, without EGR: (a) Q_c, (b) BMEP, (c) MFB_{50}, (d) $dp/d\alpha$, (e) η_{th}, (f) COV_{IMEP}, (g) t_{exh}, the volumetric share of (h) H_2O, (i) CO, (j) THC, (k) NO_x in exhaust gases, (l) PM concentration in exhaust gases.

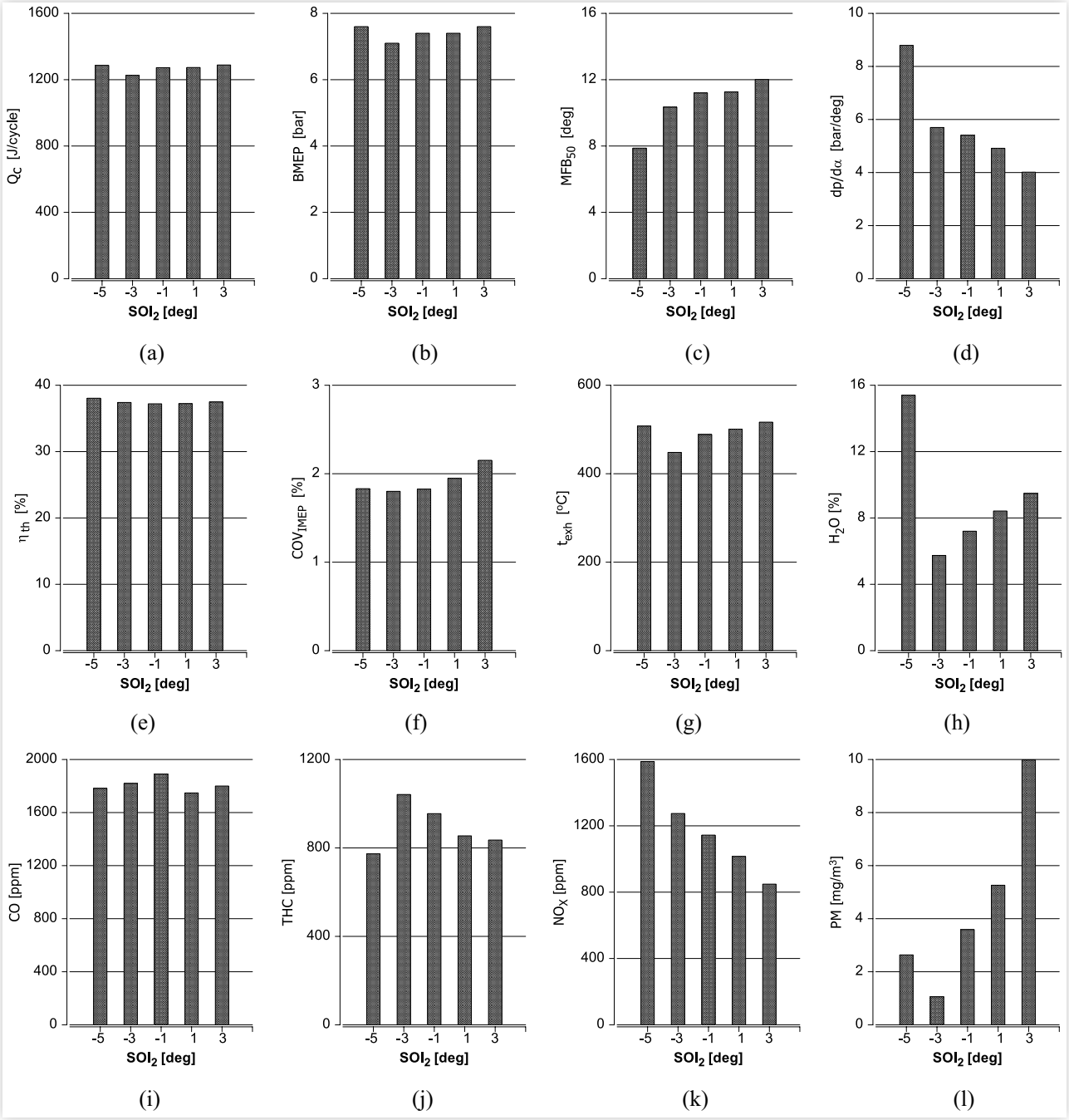

FIGURE 10 (a) Volumetric heat release rate—VHRR, (b) cylinder pressure—p, and (c) in-cylinder temperature—T diagrams with a signal from CS injector for the various SOI_2, E_{eth} = 80%, EGR (averaged diagram from data for 100 consecutive cycles).

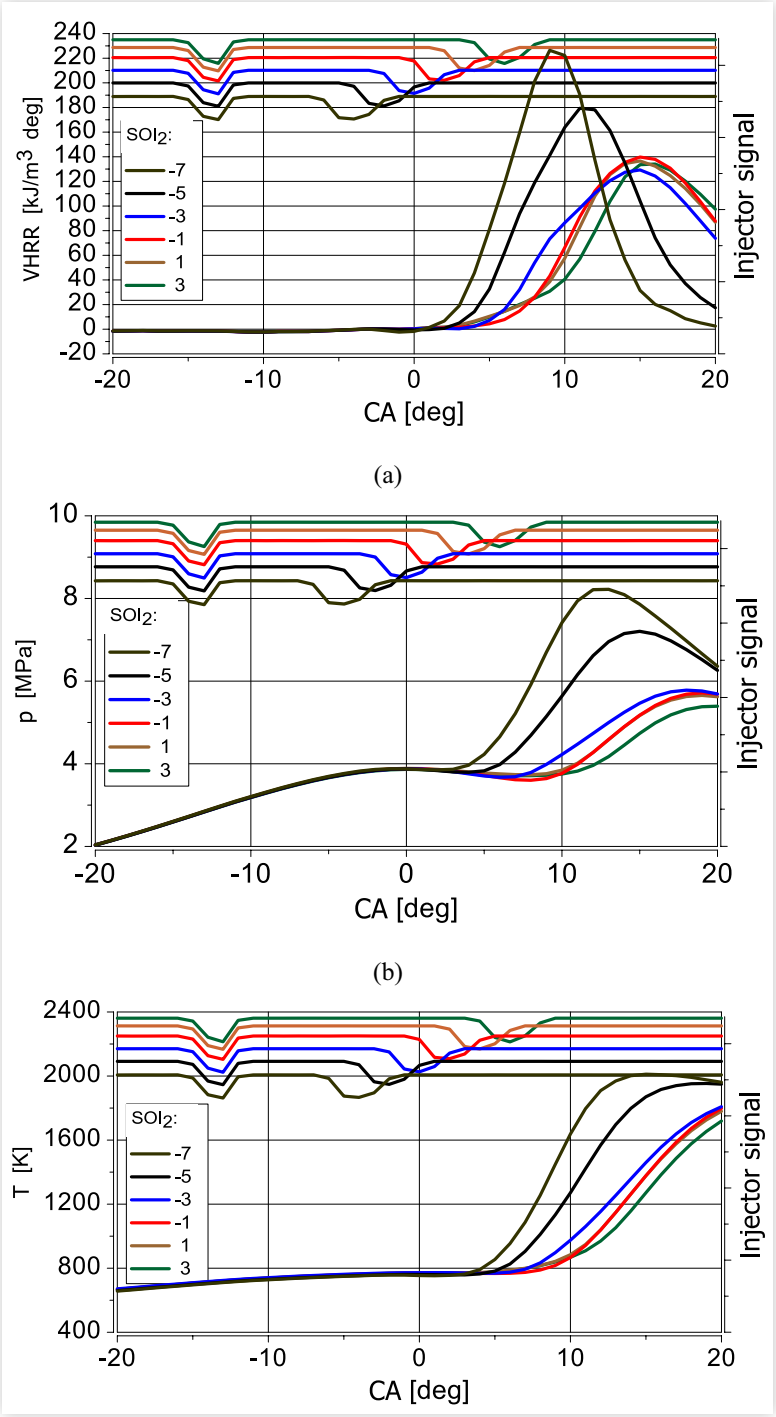

FIGURE 11 Measured and calculated engine parameters and emissions for various SOI_2, E_{eth} = 80%, EGR: (a) Q_c, (b) BMEP, (c) MFB_{50}, (d) $dp/d\alpha$, (e) η_{th}, (f) COV_{IMEP}, (g) t_{exh}, the volumetric share of (h) H_2O, (i) CO, (j) THC, (k) NO_x in exhaust gases, (l) PM concentration in exhaust gases.

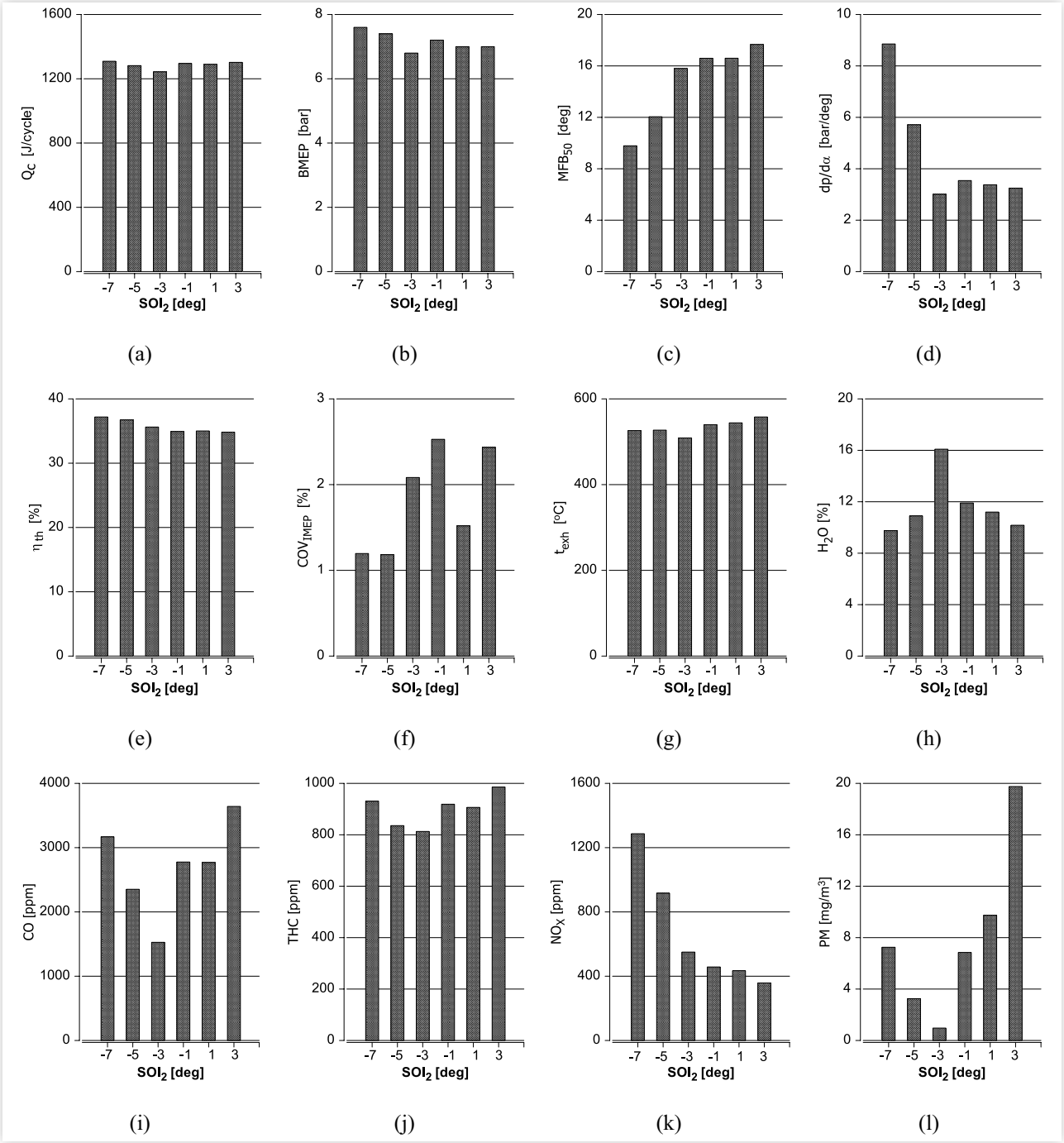

FIGURE 12 Cylinder pressure diagrams (single) registered for knock onset for combustion of DF mixture with E_{eth} = 80%: for DF mixture with EGR.

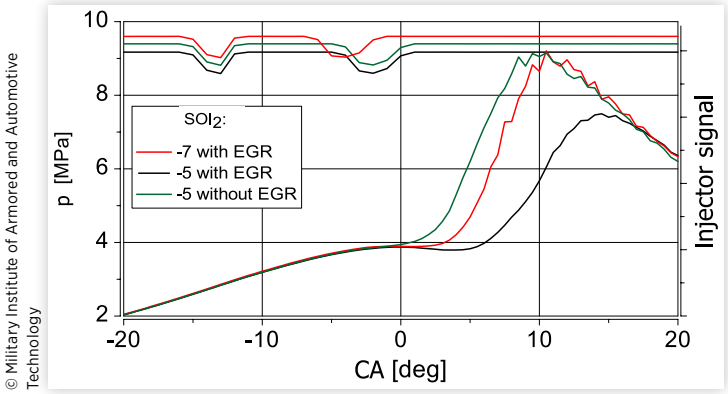

FIGURE 13 The comparison of some characteristic parameters of injection of CS and combustion of DF mixture at E_{eth} = 80% (a) EGR and (b) without EGR (yellow lines describe the injection, but red lines refer to the combustion).

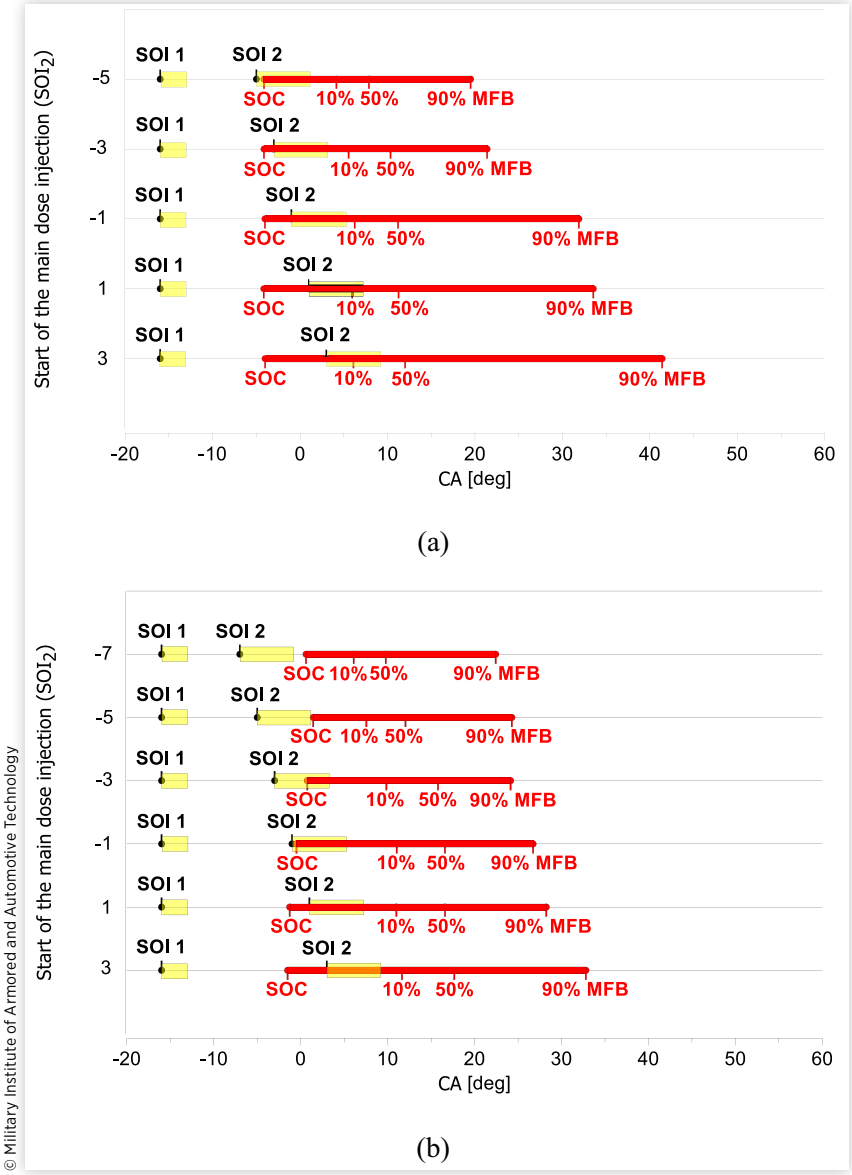

In the article, we do not deal with the durability and reliability of the engine fueled in the proposed way, including the durability test of the common rail fuel system. Still, some possible problems related to the practical application of the tested fuels are mentioned in the text.

The presented way of dual fueling of the CI engine for bio-energy generation in the future enables the use of ethanol, which can be obtained in biological or microbiological electrosynthesis (BES or MES), enabling the conversion of CO_2 into chemical energy carriers. Efficient co-burning of ethanol with renewable fuel like raw *CS* oil can also be a "new life" for the IC engine, which will find more comprehensive application in local energy production installations as an essential link in storage and energy production processes.

Contact Information

Grzegorz Pawlak, corresponding author
Military Institute of Armoured and Automotive Technology, Okuniewska 1 Street, 05-070 Sulejówek, Poland
gmpawlak07@gmail.com

Tomasz Skrzek
Kazimierz Pulaski University of Radom, Faculty of Mechanical Engineering, Chrobrego 45 Street, 26-600 Radom, Poland
t.skrzek@uthrad.pl

Krzysztof Kosiuczenko
Military Institute of Armoured and Automotive Technology, Okuniewska 1 Street, 05-070 Sulejówek, Poland
krzysztof.kosiuczenko@witpis.eu

Patryk Płochocki
Military Institute of Armoured and Automotive Technology, Okuniewska 1 Street, 05-070 Sulejówek, Poland
patryk.plochocki@witpis.eu

Przemysław Simiński
Military Institute of Armoured and Automotive Technology, Okuniewska 1 Street, 05-070 Sulejówek, Poland
przemyslaw.siminski@witpis.eu

Nomenclature

ATDC - After top dead center

BMEP - Brake mean effective pressure [bar]

BTDC - Before top dead center

CA - Crank angle [deg]

CI - Compression ignition

CO - Volumetric share of carbon monoxide in exhaust gases [%]

COV_{IMEP} - Coefficient of variation of the indicated mean effective pressure [%]

CS - Raw *Camelina sativa* oil

DF - Dual-fuel

dp/dα - Cylinder pressure rise rate [bar/deg]

E_{eth} - Substitution rate [%]

EGR - Exhaust gas recirculation

H_2O - Volumetric share of water vapor in exhaust gases [%]

HRF - High reactive fuel

IC - Internal combustion

IMEP - Indicated mean effective pressure [bar]

LHV - Lower heating value [MJ/kg]

LPA - Lean premixed autoignition

LRF - Low-reactive fuel

m - Mass [kg]

MFB_{50} - Crankshaft position where 50% of fuel mass burned over an engine cycle is reached [deg]

MFB_{90} - Crankshaft position where 90% of fuel mass burned over an engine cycle is reached [deg]

NO_x - Volumetric share of nitric oxides in exhaust gases [%]

p - Cylinder pressure [bar]

PDFC - Premixed dual-fuel combustion

PM - Particulate matter concentration in exhaust gases [mg/m^3]

PPCI - Partially premixed compression ignition

Q_c - Energy provided to the engine cylinder with the fuel per one cycle [J/cycle]

RCCI - Reactivity-controlled compression ignition

SOC - Start of combustion [deg]

SOI_1 - The start of injection of the preliminary dose of raw *Camelina sativa* oil (CS) [deg]

SOI_2 - The start of injection of the main dose of raw *Camelina sativa* oil (CS) [deg]

T - In-cylinder temperature [K]

TDC - Top dead center

t_{exh} - Exhaust temperature [°C]

THC - Volumetric share of total hydrocarbons in exhaust gases [%]

VHRR - Volumetric heat release rate [kJ/m^3 deg]

λ - Excess air coefficient [-]

$λ_{DF}$ - Total excess air coefficient for dual-fueling [-]

$η_{th}$ - Engine thermal efficiency [-]

References

1. Yergin, D., *The Quest, 'Energy, Security, and the Remaking of the Modern World'* (New York: Penguin, 2012), ISBN-10:0143121944.
2. European Council, "Fit for 55," The EU's Plan for a Green Transition, accessed December 4, 2023, https://www.

consilium.europa.eu/en/policies/green-deal/fit-for-55-the-eu-plan-for-a-green-transition/.

3. Sidibé, S.S., Blin, J., Vaitilingom, G., and Azoumah, Y., "Use of Crude Filtered Vegetable Oil as a Fuel in Diesel Engines State of the Art: Literature Review," *Renewable and Sustainable Energy Reviews* 14, no. 9 (2010): 2748-2759, doi:https://doi.org/10.1016/j.rser.2010.06.018.
4. Pawlak, G., "The Concept of a Dual-Fuel Highly Efficient Internal Combustion Engine," *SAE Int. J. Fuels Lubr.* 3, no. 2 (2010): 135-141, doi:https://doi.org/10.4271/2010-01-1480.
5. Ranganatha Swamy, L., Banapurmath, N.R., Harari, P.A., Chandrashekar, T.K. et al., "Diesel Engine Performance Fuelled with Manifold Injection of Ethanol and Water-in-Diesel Emulsion Blends," *Materials Today: Proceedings* 66 (2022): 1914-1919, doi:https://doi.org/10.1016/j.matpr.2022.05.419.
6. Gaddigoudar, P.S., Banapurmath, N.R., Basavarajappa, Y.H., Yaliwal, V.S. et al., "Effect of Injection Timing on the Performance of Ceiba Pentandra Biodiesel Powered Dual-Fuel Engine," *Materials Today: Proceedings* 49, no. 5 (2022): 1756-1761, doi:https://doi.org/10.1016/j.matpr.2021.08.009.
7. Hyunwook, P., Euijoon, S., and Choongsik, B., "Injection Strategy in Natural Gas–Diesel Dual-Fuel Premixed Charge Compression Ignition Combustion under Low Load Conditions," *Engineering* 5, no. 3 (2019): 548-557, doi:https://doi.org/10.1016/j.eng.2019.03.005.
8. Poorghasemi, K., Khoshbakhti Saray, R., Ansari, E., Khoshbakht Irdmousa, B. et al., "Effect of Diesel Injection Strategies on Natural Gas/Diesel RCCI Combustion Characteristics in a Light Duty Diesel Engine," *Applied Energy* 199 (2017): 430-446, doi:https://doi.org/10.1016/j.apenergy.2017.05.011.
9. Merts, M., Derafshzan, S., Hyvönen, J., Richter, M. et al., "An Optical Investigation of Dual-Fuel and RCCI Pilot Ignition in a Medium Speed Engine," *Fuel Communications* 9 (2021): 100037, doi:https://doi.org/10.1016/j.jfueco.2021.100037.
10. Altın, R., Çetinkaya, S., and Yücesu, H.S., "The Potential of Using Vegetable Oil Fuels as Fuel for Diesel Engines," *Energy Conversion and Management* 42, no. 5 (2001): 529-538, doi:https://doi.org/10.1016/S0196-8904(00)00080-7.
11. Koder, A., Schwanzer, P., Zacherl, F., Rabl, H.P. et al., "Combustion and Emission Characteristics of a 2.2L Common-Rail Diesel Engine Fueled with Jatropha Oil, Soybean Oil, and Diesel Fuel at Various EGR-Rates," *Fuel* 228 (2018): 23-29, doi:https://doi.org/10.1016/j.fuel.2018.04.147.
12. Mangra, A.C., Porumbel, I., and Florean, F.G., "Experimental Measurements of *Camelina sativa* Oil Combustion," *Energy for Sustainable Development* 44 (2018): 109-116, doi:https://doi.org/10.1016/j.esd.2018.03.008.
13. Pawlak, G., Płochocki, P., Simiński, P., and Skrzek, T., "The Experimental Verifcation of the Multi-Fuel IC Engine Concept with the Use of Jet Propellant-8 (JP-8) and Its Blends with Pure Rapeseed Oil," *International Journal of Energy and Environmental Engineernig* 12 (2021): 627-639, doi:https://doi.org/10.1007/s40095-021-00398-w.
14. Lebedevas, S., Klyus, O., Raslavičius, L., Krause, P. et al., "Findings on Droplet Breakup Behaviour of the Preheated Microalgae Oil Jet for Efficiency Improvement in Diesel Engines," *Biomass Conversion and Biorefinery* 13 (2022): 1-12, doi:https://doi.org/10.1007/s13399-021-02162-w.
15. Dabi, M. and Saha, U.K., "Application Potential of Vegetable Oils as Alternative to Diesel Fuels in Compression Ignition Engines: A Review," *Journal of the Energy Institute* 92, no. 6 (2019): 1710-1726, doi:https://doi.org/10.1016/j.joei.2019.01.003.
16. Pehnelt, G. and Vietze, Ch., "Uncertainties about the GHG Emissions Saving of Rapeseed Biodiesel," Jena Economic Research Paper, 2012, accessed May 11, 2024, https://www.econstor.eu/handle/10419/70134.
17. Neupane, D., Lohaus, R.H., Solomon, J.K.Q., and Cushman, J.C., "Realising the Potential of *Camelina sativa* as a Bioenergy Crop for a Changing Global Climate," *Plants* 11 (2022): 772, doi:https://doi.org/10.3390/plants11060772.
18. Murphy, E.J., "Chapter 8: Camelina (*Camelina sativa*)," in McKeon, T.A., Hayes, D.G., Hildebrand, D.F., and Weselake, R.J. (eds.), *Industrial Oil Crops* (Elsevier, Amsterdam: OCS Press, 2016), 207-230, https://doi.org/10.1016/B978-1-893997-98-1.00008-7.
19. Aslam, M.M., Usama, M., Nabi, H.G., Ahmad, N. et al., "*Camelina sativa* Biodiesel Cope the Burning Issue of Global Worming; Current Status and Future Predictions," *Modern Concepts & Developments in Agronomy* 3, no. 5 (2019): 358-361, doi:https://doi.org/10.31031/mcda.2019.03.000573.
20. Chaturvedi, S., Bhattacharya, A., Khare, S.K., and Kaushik, G., "*Camelina sativa*: An Emerging Biofuel Crop," in Hussain, C.M. (ed.), *Handbook of Environmental Materials Management* (Cham, Switzerland: Springer International Publishing, 2018), 1-38, https://doi.org/10.1007/978-3-319-73645-7_110.
21. Gesch, R.W., Isbell, T.A., Oblath, E.A., Allen, B.L. et al., "Comparison of Several *Brassica* Species in the North Central U.S. for Potential Jet Fuel Feedstock," *Industrial Crops and Products* 75 (2015): 2-7, doi:https://doi.org/10.1016/j.indcrop.2015.05.084.
22. Owczuk, M. and Kołodziejczyk, K., "Assessment of the Possibility of Using Straw and Pomace of *Camelina sativa* as an Alternative Energy Source," *Chemik* 65, no. 6 (2011): 537-542.
23. Achinas, S., Jan, G., and Euverink, W., "Consolidated Briefing of Biochemical Ethanol Production from Lignocellulosic Biomass," *Electronic Journal of Biotechnology* 23 (2016): 44-53, doi:https://doi.org/10.1016/j.ejbt.2016.07.006.
24. Bajpai, P., "Global Production of Bioethanol," in Bajpal, P. (ed.), *Developments in Bioethanol*, Green Energy and Technology (Singapore: Springer, 2021), 177-196, https://doi.org/10.1007/978-981-15-8779-5.
25. Taghizadeh-Alisaraei, A., Motevali, A., and Ghobadian, B., "Ethanol Production from Date Wastes: Adapted Technologies, Challenges, and Global Potential," *Renewable Energy* 143 (2019): 1094-1110, doi:https://doi.org/10.1016/j.renene.2019.05.048.

26. Chen, H. and Wang, L., "Chapter 6: Sugar Strategies for Biomass Biochemical Conversion," in Chen, H. and Wang, L. (eds.), *Technologies for Biochemical Conversion of Biomass* (London, UK: Academic Press, 2017), 137-164, https://doi.org/10.1016/B978-0-12-802417-1.00006-5.
27. Voegele, E., "Report: EU Ethanol Consumption to Increase in 2019," *Ethanol Producer Magazine*, accessed March 1, 2024, http://ethanolproducer.com/articles/16422/report-eu-ethanol-consumption-to-increase-in-2019.
28. GlobeNewswire, "EU Ethanol Market Report: Suppliers, Prices, Trends and Forecast to 2030—IndexBox," accessed March 1, 2024, https://www.globenewswire.com/news-release/2022/05/31/2452969/0/en/EU-Ethanol-Market-Report-Suppliers-Prices-Trends-and-Forecast-to-2030-IndexBox.html.
29. Kim, S. and Dale, B.E., "Global Potential Bioethanol Production from Wasted Crops and Crop Residues," *Biomass and Bioenergy* 26, no. 4 (2004): 361-375, doi:https://doi.org/10.1016/j.biombioe.2003.08.002.
30. Muchez, L., De Vos, D.E., and Kim, M., "Sacrificial Anode-Free Electrosynthesis of α-Hydroxy Acids via Electrocatalytic Coupling of Carbon Dioxide to Aromatic Alcohols," *ACS Sustainable Chemistry & Engineering* 7, no. 19 (2019): 15860-15864, doi:https://doi.org/10.1021/acssuschemeng.9b04612.
31. Budnikova, Y.H., Dolengovski, E.L., Tarasov, M.V. et al., "Electrochemistry in Organics: A Powerful Tool for 'Green' Synthesis," *Journal of Solid State Electrochemistry* 28, no. 3 (2024): 659-676, doi:https://doi.org/10.1007/s10008-023-05507-9.
32. Arshad, M., *Sustainable Ethanol and Climate Change. Sustainability Assessment for Ethanol Distilleries* (Cham, Switzerland: Springer Nature Switzerland AG, 2021), doi:https://doi.org/10.1007/978-3-030-59280-6
33. Arshad, M., *Perspectives on Water Usage for Biofuels Production: Aquatic Contamination and Climate Change* (Cham, Switzerland: Springer International Publishing, 2017), doi:https://doi.org/10.1007/978-3-319-66408-8
34. Manteuffel Szoege, H. and Wiśniewski, M., "Ekologiczne i ekonomiczne aspekty produkcji etanolu energetycznego w małych gorzelniach rolniczych," *Inżynieria Rolnicza (Agricultural Enginnering)* 2, no. 143 (2013): 215-224 (in Polish).
35. Taasevigen, D.J., "*Camelina* Composite Pellet Fuels Feasibility for Residential and Commercial Applications," MS thesis, Montana State University - Bozeman, College of Engineering, 2013.
36. Dangol, N., Shrestha, D., and Duffield, J.A., "Life Cycle Analysis and Production Potential of *Camelina* Biodiesel in the Pacific Northwest," *Transactions of the American Society of Agricultural and Biological Engineers* 58, no. 2 (2015): 465-475, doi:https://doi.org/10.13031/trans.58.10771.
37. Dierickx, J., Verbiest, J., Janvier, T., Peeters, J. et al., "Retrofitting a High-Speed Marine Engine to Dual-Fuel Methanol-Diesel Operation: A Comparison of Multiple and Single Point Methanol Port Injection," *Fuel Communications* 7 (2021): 100010, doi:https://doi.org/10.1016/j.jfueco.2021.100010.
38. Waraich, E., Ahmed, Z., Ahmad, R., Ashraf, M. et al., "*Camelina sativa*, a Climate Proof Crop, Has High Nutritive Value and Multiple-Uses: A Review," *Australian Journal of Crop Science* 7 (2013): 1551-1559.
39. Aralu, C.E., Eseoghene Karakitie, D., and Abimbola Fadare, D., "Construction of a Pilot Scale Biogas Digester at the University of Ibadan Dairy Farm, Abadina," *Fuel Communications* 9 (2021): 100033, doi:https://doi.org/10.1016/j.jfueco.2021.100033.
40. Park, H., Shim, E., and Bae, C., "Improvement of Combustion and Emissions with Exhaust Gas Recirculation in a Natural Gas-Diesel Dual-Fuel Premixed Charge Compression Ignition Engine at Low Load Operations," *Fuel* 235 (2019): 763-774, doi:https://doi.org/10.1016/j.eng.2019.03.005.
41. Pawlak, G. and Skrzek, T., "Combustion of Raw *Camelina sativa* Oil in CI Engine Equipped with Common Rail System," *Scientific Reports* 13 (2023): 19731, doi:https://doi.org/10.1038/s41598-023-46613-y.
42. Wartsila, "Combustion Engine for Power Generation: Introduction," accessed August 22, 2023, https://www.wartsila.com/energy/learn-more/technology-comparison-engine-vs-aero/combustion-engine-for-power-generation-introduction.
43. May, I., Pedrozo, V., Zhao, H., Cairns, A. et al., "Characterisation and Potential of Premixed Dual-Fuel Combustion in a Heavy Duty Natural Gas/Diesel Engine," SAE Technical Paper 2016-01-0790 (2016), doi:https://doi.org/10.4271/2016-01-0790.
44. Martin, J., Boehman, A., Topkar, R., Chopra, S. et al., "Intermediate Combustion Modes between Conventional Diesel and RCCI," *SAE Int. J. Engines* 11, no. 6 (2018): 835-860, doi:https://doi.org/10.4271/2018-01-0249.
45. Martin, J. and Boehman, A., "Mapping the Combustion Modes of a Dual-Fuel Compression Ignition Engine," *International Journal of Engine Research* 23, no. 9 (2021): 1453-1474, doi:https://doi.org/10.1177/14680874211018376.
46. Ickes, A., Hanson, R., and Wallner, T., "Impact of Effective Compression Ratio on Gasoline-Diesel Dual-Fuel Combustion in a Heavy-Duty Engine Using Variable Valve Actuation," SAE Technical Paper 2015-01-1796 (2015), doi:https://doi.org/10.4271/2015-01-1796.
47. Crawford, M., "The Power of Dual-Fuel Diesel Engines," ASME.org, accessed August 21, 2023, https://www.asme.org/topics-resources/content/power-of-dualfuel-diesel-engines.
48. Kashipura, N., Banapurmath, N.R., Manavendra, G., Nagaraj, A.M. et al., "Effect of Combustion Chamber Shapes on the Performance of Duel Fuel Engine Operated on Rice Bran Oil Methyl Ester and Producer Gas," *Journal of Petroleum and Environmental Biotechnology* 6 (2015): 4, 1-8, doi:https://doi.org/10.4172/2157-7463.1000225.
49. Di Blasio, G., Belgiorno, G., and Beatrice, C., "Effects on Performances, Emissions and Particle Size Distributions of a

Dual-Fuel (Methane-Diesel) Light-Duty Engine Varying the Compression Ratio," *Applied Energy* 204 (2017): 726-740, doi:https://doi.org/10.1016/j.apenergy.2017.07.103.

50. Yin, C.B., Zhang, Z.D., Xie, N.L., Sun, Y.D. et al., "Knock in Dual-Fuel Diesel Combustion with an E85 Ethanol/Gasoline Blend by Multi-Dimensional Simulation," *International Journal of Automotive Technology* 17 (2016): 591-604, doi:https://doi.org/10.1007/s12239-016-0059-0.
51. Lounici, M.S., Benbellil, M.A., Loubar, K., Niculescu, D.C. et al., "Knock Characterisation and Development of a New Knock Indicator for Dual-Fuel Engines," *Energy* 141 (2017): 2351-2361, doi:https://doi.org/10.1016/j.energy.2017.11.138.
52. Kassa, M. and Hall, C., "Dual-Fuel Combustion," in Carlucci, A.P. (ed.), *The Future of Internal Combustion Engines* (London: IntechOpen, 2018), doi:https://doi.org/10.5772/intechopen.80570.
53. Zhong, Q., Shen, H., Yun, X., Chen, Y. et al., "Global Sulfur Dioxide Emissions and the Driving Forces," *Environmental Science and Technology* 54, no. 11 (2020): 6508-6517, doi:https://doi.org/10.1021/acs.est.9b07696.
54. Scania, "Scania's Bioethanol Engine Reduces CO_2 Emissions," accessed August 21, 2023. https://www.scania.com/group/en/home/newsroom/news/2018/scanias-bioethanol-engine-reduces-CO2-emissions.html.
55. Belgiorno, G., Di Blasio, G., Shamun, S., Beatrice, C. et al., "Performance and Emissions of Diesel-Gasoline-Ethanol Blends in a Light Duty Compression Ignition Engine," *Fuel* 217 (2018): 78-90, doi:https://doi.org/10.1016/j.fuel.2017.12.090.
56. Sarjovaara, T., Alantie, J., and Larmi, M., "Ethanol Dual-Fuel Combustion Concept on Heavy Duty Engine," *Energy* 63 (2013): 76-85, doi:https://doi.org/10.1016/j.energy.2013.10.053.
57. Di Blasio, G., Beatrice, C., and Molina, S., "Effect of Port Injected Ethanol on Combustion Characteristics in a Dual-Fuel Light Duty Diesel Engine," SAE Technical Paper 2013-01-1692 (2013), doi:https://doi.org/10.4271/2013-01-1692.
58. Yıldızhan, Ş. and Serin, H., "Biodiesel Production from False Flax (*Camelina sativa*) Oil and Its Blends with Diesel Fuel," *The Journal of MacroTrends in Energy and Sustainability* 3, no. 1 (2015): 24-30.
59. Aydogan, H., Ozcelik, A.E., and Acaroglu, M., "An Experimental Study of the Effects of *Camelina sativa* Biodiesel-Diesel Fuel on Exhaust Emissions in a Turbocharged Diesel Engine," *Journal of Clean Energy Technologies* 5, no. 3 (2017): 254-257, doi:https://doi.org/10.18178/jocet.2017.5.3.378.
60. Orlen, "Ekodiesel Ultra," 2021, accessed August 20, 2023, https://www.orlen.pl/EN/ForBusiness/Fuel/Diesel/Pages/EkodieselUltra.aspx.
61. Wu, Y., Zhang, X., Zhang, Z., Wang, X. et al., "Effects of Diesel-Ethanol-THF Blend Fuel on the Performance and Exhaust Emissions on a Heavy-Duty Diesel Engine," *Fuel* 271 (2020): 117633, doi:https://doi.org/10.1016/j.fuel.2020.117633.
62. Single Cylinder Research Engine 5405, "User's Guide," Radom University, AVL AT5472E Rev.00, 2013.
63. Skrzek, T. et al., "Repeatability of High-Pressure Measurement in a Diesel Engine Test Bed," *Sensors* 20 (2020): 3478, doi:https://doi.org/10.3390/s20123478.
64. Heywood, J., *Internal Combustion Engines Fundamentals* (New York: McGraw-Hill, 1988), ISBN:9780070286375
65. Zhu, J., Li, J., Wang, S., Raza, M. et al., "Ignition Delay Time Measurements and Kinetic Modeling of Methane/Diesel Mixtures at Elevated Pressures," *Combustion and Flame* 229 (2021): 111390, doi:https://doi.org/10.1016/j.combustflame.2021.02.036.